AIChE

Determining Fouling-Independent Component of Critical Flux in Protein Ultrafiltration Using the Free-Solvent-Based (FSB) Model

Yiheng Wang and V. G. J. Rodgers
B2K Group (Biotransport and Bioreaction Kinetics Group), Dept. of Bioengineering, A237 Bourns Hall, 900 University Ave, University of California, Riverside, CA 92521

DOI 10.1002/aic.12152
Published online February 19, 2010 in Wiley Online Library (wileyonlinelibrary.com).

Keywords: critical flux, limiting flux, osmotic pressure, free-solvent-based (FSB) model, protein ultrafiltration

Introduction

In protein ultrafiltration (UF), critical flux is generally considered the point on the flux-pressure curve where the permeate flux begins to significantly deviate from the pure solvent flux line. This concept has generally been associated with membrane fouling. Recently, however, we showed that a free-solvent-based model (FSB model) demonstrated that osmotic pressure can be the primary and dominant factor for the nonlinear flux behavior observed in protein UF. Consequently, the critical flux may be the results of two phenomena, the osmotic pressure effect and potential irreversible fouling. Here we show that the fouling-independent component of the critical flux can be redefined as the critical point of the second derivative of the flux-pressure profile determined from the FSB model. This definition of the fouling-independent component of critical flux was compared to values traditionally determined qualitatively on the flux-pressure curve and was found to be in excellent agreement with these experimental observations.

During protein ultrafiltration (UF), critical flux has been generally considered the mark of the deviation of the permeate flux from the linear pressure dependence of the pure solvent flux. It has been defined as the flux below which no fouling occurs.[1] Critical flux has seen growing interest from the researchers over the past 10 years due to the importance in understanding the nonlinear flux-pressure dependence during UF processes.[2–8] Bacchin et al.[1] recently published a comprehensive review that summarizes the research on the critical flux. Despite the variation in theories, experimental methods, and mathematical models developed by different researchers, the general agreement is that the nonlinear flux behavior is the result of the hydraulic resistance associated with various membrane fouling phenomena. Hence, a family of critical fluxes (strong form, weak form, and critical flux for irreversibility) is defined based on different types of fouling behaviors.

Recently, we have developed a new flux model, the free-solvent-based (FSB) model (based on the free-solvent model for osmotic pressure[9–13]).The free-solvent model for concentrated solutions has been around of some time but has, surprisingly been overlooked for its application to concentrated protein solutions. As early as 1916, Frazer and Myrick[14] analyzed the nonidealities in aqueous sucrose solutions using a free-solvent model. More recently, other researchers, in a similar approach, based their models on the van't Hoff equation, but only had limited success for protein solutions up to moderate concentrations.[15–18] However, we have subsequently demonstrated that a free-solvent model corrected for ion binding demonstrates excellent predictability for osmotic pressure of concentrated solutions of lysozyme, ovalbumin, albumin and immunogamma- globulins in a range of moderate salt solutions with varying pH. In fact, the free-solvent model demonstrated excellent prediction for protein concentrations up to saturation concentrations.

We have recently shown that this model provides excellent prediction and characterization of the flux-pressure behavior in protein UF.[19] We further showed that when membrane fouling contributions are experimentally minimized, the permeate flux continues to demonstrate nonlinear, reversible pressure dependence, and reaches limiting flux at sufficiently high pressure. These observations are in excellent agreement with the FSB model prediction. The unique feature of the free-solvent model for this work is that one

Correspondence concerning this article should be addressed to V. G. J. Rodgers at victor.rodgers@ucr.edu.

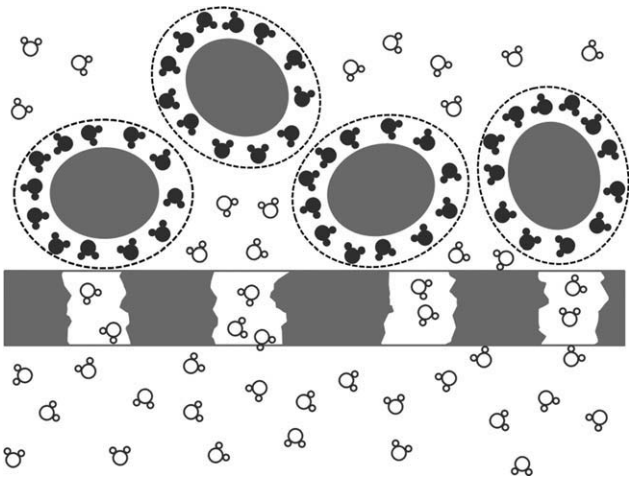

Figure 1. Schematic diagram of the membrane region that illustrates the concept of the hydration effects during protein UF.

The molecules within each dashed ellipse represent a single hydrated protein in the free-solvent model. The water molecules that bind to the proteins have different chemical potential than those unbound, *free* water molecules, therefore, only the water molecules outside the dashed lines are considered as solvent. When the van Laar equation is invoked to calculate the osmotic pressure, only the mole fractions of the *free* water should be considered.

can relax the membrane fouling dominant contribution, and still successfully predict and characterize the flux behavior for the entire pressure range through the limiting flux region. The FSB model also reveals that nonlinear flux behavior exists due to the highly nonlinear variation of osmotic pressure in highly concentrated solutions, which are inevitable at the membrane wall during UF. Thus, a natural consequence of the response of osmotic pressure to the increase in applied hydraulic pressure is that it will dramatically affect the flux-pressure behavior in protein UF, regardless of fouling. Thus, it is advantageous to decouple the effects of osmotic pressure when evaluating the onset of critical flux. The FSB model provides the appropriate approach to do this.

Figure 1 is a schematic diagram of the membrane region that illustrates the concept of the hydration effects during protein UF. The molecules within each dashed ellipse represent a single hydrated protein in the free-solvent model. Since water molecules that bind to the protein have altered chemical potential with respect to *free* water molecules, only the mole fractions of the *free* water should be considered when the van Laar equation is invoked to calculate the osmotic pressure.

The objective of this work is to examine the fouling-independent component of critical flux in protein UF in the framework of the FSB model and compare these results to observed critical flux behavior.

Experimental observations

Limiting flux experiments have been reported and analyzed previously.[19] Briefly, flux results from cross-flow ultrafiltration experiments (shear rate of 116 s^{-1}) of moderate ionic strength (0.15 M NaCl) solutions of ovalbumin (OVA), bovine serum albumin (BSA) and immuno-gamma globulin (IgG) were determined for various operating pressures and pH. Nonlinear flux-pressure behavior, as well as the approach to limiting flux was observed in all experiments. Composite regenerated cellulose (CRC, 30 kDa MWCO, Millipore, Bedford, MA) was used for this work. CRC membranes are recognized for their low extent of membrane fouling. Additional membrane fouling effect was minimized by using preconditioned membranes that had been soaked in the corresponding protein feed solutions. The hydraulic permeability of all conditioned membranes were within the error range of that of the fresh membrane (n = 32 cases), and the change between the pre- and post-experimental hydraulic permeability was consistently less than 10%. In addition, the observed flux behavior demonstrated strong reversibility, confirming that we were observing the fouling-independent component of flux.

FSB model calculation

As pointed out previously,[19] permeate flux is calculated by the FSB model that uses the Kedem-Katchalsky model (Eq. 1),[20] film theory (Eq. 2),[21] and the free-solvent representation for osmotic pressure (Eq. 3)[9–13]:

$$J_v = L_p(\Delta P - \sigma\Delta\pi), \tag{1}$$

$$J_v = k\ln\left(\frac{C_w - C_p}{C_b - C_p}\right), \tag{2}$$

and

$$\Delta\pi = -\frac{RT}{\bar{V}_1}\ln\frac{x^f_{1,w}}{x^f_{1,p}}. \tag{3}$$

In Eq. 3, the osmotic pressure across the membrane $\Delta\pi$, is calculated following the van Laar equation, with $x^f_{1,w}$ and

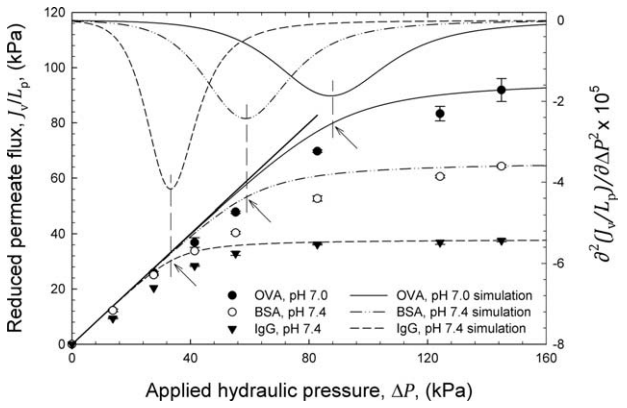

Figure 2. Experimental data and model simulation.

The symbols represent the experimental results of UF experiments for OVA (at pH 7.0), BSA (at pH 7.4) and IgG (at pH 7.4) in moderate NaCl solution. All flux results were reduced by the pre-experimental hydraulic permeability for each experiment. The curve on each data set is the simulation curve calculated by the FSB model. The respective second derivative $\frac{\partial^2(J_v/L_p)}{\partial\Delta P^2}$ vs. ΔP, for each case is also plotted on the same plot. The critical point of the second derivative defines the fouling-independent critical flux on the flux-pressure curve, and each corresponding critical flux is noted by arrows.

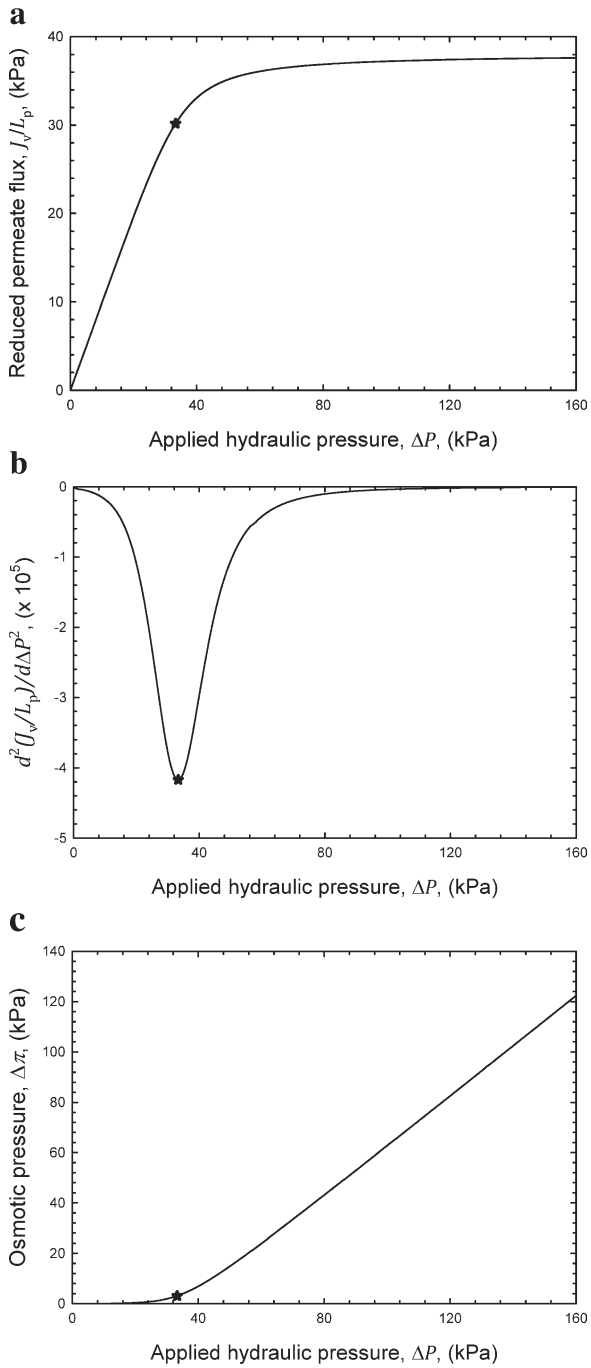

Figure 3. Graphical illustrations of fouling-independent critical flux using the simulation of the experiment of IgG at pH 7.4 as an example.

The critical point that defines the fouling-independent critical flux is represented in each plot by the star symbol. Figure 3a is the J_v/L_p vs. ΔP plot. Figure 3b is the $\frac{\partial^2(J_v/L_p)}{\partial\Delta P^2}$ vs. ΔP plot, with the point of the fouling independent critical flux being the critical point of the curve. Figure 3c is the $\Delta\pi$ vs. ΔP plot, and the point of fouling-independent critical flux marks the point where osmotic pressure becomes significant and competitive to the applied hydraulic pressure. Figure 3c can be interpreted as the $[J_v(\text{solvent}) - J_v]$ vs. ΔP plot, and it simultaneously represents the behavior of the permeate flux deviation from the pure solvent flux, since $\Delta\pi = \frac{J_v(\text{solvent})}{L_p} - \frac{J_v}{L_p}$ (with σ modeled as 1).

$x^f_{1,p}$ being the mole fractions of *free* water at the membrane wall, and in the permeate flux, respectively. At each chosen pressure, the permeate flux is calculated through iteration. This procedure is applied to the entire flux-pressure range through the limiting flux region. The detailed discussion of the FSB model can be found in Wang and Rodgers.[19] It should be pointed out that the aforementioned theoretical procedure does not take into consideration of any membrane fouling contribution and is focused on the fouling-independent contributions to flux.

Simulation curves calculated by the FSB model are plotted with experimental data (OVA at pH 7.0, BSA at pH 7.4 and IgG at pH 7.4, represented by symbols) in Figure 2. The mass-transfer coefficients used in the calculations were determined by regression on the last data point (which corresponds to the highest protein wall concentration) of each data set. As Figure 2 shows, the FSB model not only predicts limiting flux, but it also provides excellent characterization of the nonlinear flux-pressure behavior.

Definition of fouling-independent critical flux: model calculation and discussion

From these results we can define the fouling-independent critical flux as the flux at the critical point of the second derivative of the FSB flux-pressure profile. This definition is also illustrated in Figure 2. In Figure 2, the simulation curves of J_v/L_p vs. ΔP function were plotted together with the respective second derivative $\frac{\partial^2(J_v/L_p)}{\partial\Delta P^2}$ vs. ΔP. All derivatives were calculated numerically using the backward finite difference method. The corresponding points where the critical fluxes occur according to the new definition are noted by arrows. As Figure 2 shows, the critical flux defined by this method is comparable to the qualitative definition of fouling-independent critical flux corresponding to deviation of the flux-pressure curve from the solvent flux line.

The simulation of the experiment of IgG at pH 7.4 is used here as an example for further discussion of the new definition for the critical flux. Different graphical illustrations for the defined critical point are summarized in Figure 3a–c, and they are J_v/L_p vs. ΔP plot, $\frac{\partial^2(J_v/L_p)}{\partial\Delta P^2}$ vs. ΔP plot, and $\Delta\pi$ vs. ΔP plot, respectively. The critical point that defines the critical flux was also represented in each plot by the star symbol. As Figure 3c shows, the physical meaning of the fouling-independent critical flux, defined this way, marks the point where osmotic pressure begins to become significant and competitive to the applied hydraulic pressure. Figure 3c, simultaneously, represents the behavior of the permeate flux deviation from the pure solvent flux $J_v(\text{solvent}) - J_v$, since with the assumptions of constant L_p, $\frac{J_v(\text{solvent})}{L_p} = \Delta P$ and $\frac{J_v}{L_p} = \Delta P - \Delta\pi$ (with σ modeled as 1) are invoked. When Figure 3c is interpreted as the $[J_v(\text{solvent}) - J_v]$ vs. ΔP plot, it provides a comparable definition to the marked point when the flux-pressure behavior first becomes nonlinear, since as Figure 3c shows, below fouling-independent critical flux, the difference between $J_v(\text{solvent})$ and J_v is observably negligible.

Conclusion

In this work, the concept of critical flux is revisited through the FSB model for the permeate flux in protein UF.

It is observed that critical flux may be the results of the combination of a fouling and a fouling-independent component. Here we have use a free-solvent-based osmotic pressure model (FSB) to decouple the fouling-independent component of critical flux. Furthermore, we have shown that the FSB model provides a mathematical definition of the fouling-independent critical flux as the ''critical point'' of the second derivative of the flux-pressure profile. The physical meaning of the fouling-independent critical flux defined this way is that it marks the point where osmotic pressure starts to become significant and competitive to the applied hydraulic pressure. Finally, we have shown that this prediction for fouling-independent critical flux is in excellent agreement with the qualitative observed point of critical flux for prefouled membranes.

Acknowledgments

We wish to acknowledge the funding support from NSF grant award No. 0091552.

Notation

J_v = volumetric permeate flux, m/s
k = solute mass-transfer coefficient, m/s
L_p = hydraulic permeability, m/s-Pa
x_i = molar fraction of species i
ΔP = transmembrane hydraulic pressure, kPa
R = ideal gas constant, 8.314 J/mol-K
T = temperature, K
$\overline{V}_i$ = partial molar volume of species i, m^3/mol

Greek letters

$\Delta\pi$ = transmembrane osmotic pressure, kPa
σ = reflection coefficient

Superscripts

I = phase I
II = phase II
f = free solvent

Subscripts

1 = water
w = membrane wall
p = permeate

Literature Cited

1. Bacchin P, Aimar P, Field RW. Critical and sustainable fluxes: Theory, experiments and applications. *J Membr Sci*. 2006;281:42–69.
2. Field RW, Wu D, Howell JA, Gupta BB. Critical flux concept for microfiltration fouling. *J Membr Sci*. 1995;100:259–272.
3. Howell JA. Sub-critical flux operation of microfiltration. *J Membr Sci*. 1995;107:165–171.
4. Bacchin Aimar P, Sanchez V. Model for colloidal fouling of membranes. *AIChE J*. 1995;41:368–377.
5. Wu D, Howell JA, Field RW. Critical flux measurement for model colloids. *J Membr Sci*. 1999;152:89–98.
6. Bacchin P. A possible link between critical and limiting flux for colloidal systems: consideration of critical deposit formation along a membrane. *J Membr Sci*. 2004;228:237–241.
7. Metsämuuronen S, Nyström M. Critical flux in cross-flow ultrafiltration of protein solutions. *Desalination*. 2005;175:37–47.
8. Chiu TY, Lara Dominguez MV, James AE. Critical flux and rejection behaviour of non-circular-channelled membranes: Influence of some operating conditions. *Sep Purif Technol*. 2006;50:212–219.
9. Yousef MA, Datta R, Rodgers VGJ. Free-solvent model of osmotic pressure revisited: application to concentrated IgG solution under physiological conditions. *J Colloid Interface Sci*. 1998;197:108–118.
10. Yousef MA, Datta R, Rodgers VGJ. Understanding nonidealities of the osmotic pressure of concentrated bovine serum albumin. *J Colloid Interface Sci*. 1998;207:273–282.
11. Yousef MA, Datta R, Rodgers VGJ. Confirmation of free solvent model assumptions in predicting the osmotic pressure of concentrated globular proteins. *J Colloid Interface Sci*. 2001;243:321–325.
12. Yousef MA, Datta R, Rodgers VGJ. Monolayer hydration governs nonideality in osmotic pressure of protein solutions. *AIChE J*. 2002;48:1301–1308.
13. Yousef MA, Datta R, Rodgers VGJ. Model of osmotic pressure for high concentrated binary protein solutions. *AIChE J*. 2002;48:913–917.
14. Frazer JC, Myrick RT. The osmotic pressure of sucrose solution at 30°. *J Am Chem Soc*. 1916;38(10):1907–1922.
15. Ling GN, Ochsenfeld MM, Walton C, Bersinger TJ. Mechanism for solute exclusion from cells: the role of protein-water interaction. *Physiol Chem Phys*. 1980;12:3–10.
16. Ling GN. *In Search of the Physical Basis of Life*. New York: Plenum Press; 1984.
17. Cameron IL, Fullerton GD. A model to explain the osmotic pressure behavior of hemoglobin and serum albumin. *Biochem Cell Biol*. 1990;68:894–898.
18. Fullerton GD. Zimmerman RJ, Cantu C, Cameron IL. New expression to describe solution nonideal osmotic pressure, freezing point depression and vapor pressure. *Biochem Cell Biol*. 1992;70:1325–1331.
19. Wang Y, Rodgers VGJ. Free-solvent model shows osmotic pressure dominates the limiting flux in protein ultrafiltration. *J Membr Sci*. 2008;320:335–343.
20. Kedem O, Katchalsky A. Thermodynamic analysis of the permeability of biological membranes to non-electrolytes. *Biochim Biophys Acta*. 1958;27:229–246.
21. Michaels AS. Separation technique for the CPI (chemical process industry). *Chem Eng Prog*. 1968;64:31–43.

Manuscript received Aug. 17, 2009, and revision received Nov. 17, 2009.